Noether's Theorem on Non-Trivial Manifolds

Daniel Martin

Department of Physics, University of Warwick, Coventry CV4 7AL, United Kingdom

13/03/2014

Noether's theorem has been used to great success throughout many areas of physics, and has been one of the main generators of new research areas. This paper extends her results to general Manifolds and finds the necessary conditions for her theorem to break down. The example of the Möbius strip is investigated in detail and by the inclusion of Complex numbers in it's structure, leads to possibilities of generating Quantum Theory merely from structurally abstract space-times.

1 Introduction

One of the most resilient theories in Physics is that of Hamilton's Principle, the idea that any system will evolve in such a way as to minimise it's action. This, originally formulated as an equivalent explanation of Newtonian mechanics has survived throughout the revolutions of Relativity and Quantum Mechanics. Alongside this lies the famous Noether's theorem. When Emmy Noether published her theorem in 1918 [1], she released one of the most powerful tools into the world of physics. In words, this is a theorem regarding the correspondence between symmetries and conservation laws present in a system, in mathematics it becomes even more elegant, it intertwines Group Theory to Quantum Mechanics and essentially creates the field of Particle Physics.

The motivation for this project comes, as much physics does, from an example. Consider a particle moving on a Möbius strip. If only its local motion is examined, the strip is viewed as a flat surface equivalent to $\mathbb{R}^2$, and hence local translational symmetry is present and by a standard result from Noether, two conserved momenta are obtained. Now if global motion is considered, e.g. the particle making one rotation around the loop with some velocity perpendicular to the loop, it can be seen that upon returning to the initial loop position, the perpendicular velocity has been reversed. This immediately shows that at least one component of momentum is not always conserved, clearly there is something beneath this effect, some description of the system that has not been studied and is not accounted for in the initial theorem.

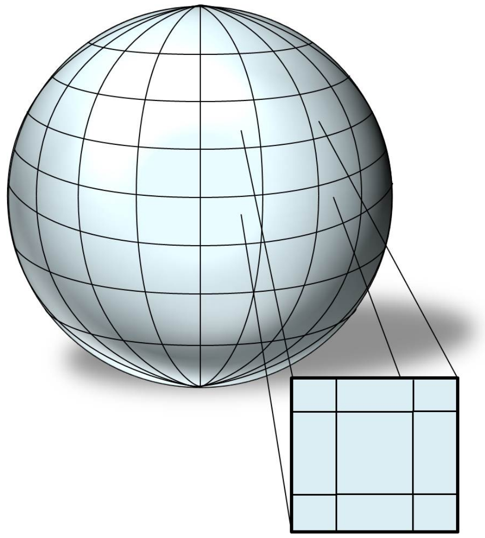

Figure 1: The Sphere $\mathbb{S}^2$ is locally equivalent to $\mathbb{R}^2$.

2 Theory

2.1 Manifolds

2.1.1 Structure of Manifolds

The starting point for any exploration of non-trivial motion is the Mathematical Topic of Manifolds. An intuitive idea of a manifold is some space that is locally equivalent to $\mathbb{R}^n$, as an example if a small portion of the surface of a sphere is examined then this can and will be assumed to be flat, as one experiences living on the Earth, this is shown in Figure 1. This way of thinking is helpful when trying to gain some understanding of the system, but the mathematical description must be explored to acquire satisfying and rigorous answers. As an example consider two lines crossing each other and ask the question, “Is this a manifold?” It could be said that this is locally equivalent to $\mathbb{R}$, but as will be seen shortly, there are further conditions which are broken with this example. To start the theory, Topology must be visited briefly.

Definition 1 *Given a set S, and, τ, a collection of subsets of S. τ is called a topology on S if the following 3 criteria hold:*

- $\emptyset, S \in \tau$
- $\forall\ T_i \in \tau,\ \bigcup_{i=1}^{\infty} T_i \in \tau$
- $\bigcap_{i=1}^{n} T_i \in \tau, n \in \mathbb{N}$

When these conditions are satisfied the pair (S, τ) is termed a Topological space, and the elements of τ are defined to be open. This creates the most general structure you can put on a set, since it only requires the concepts of subsets and does not need more intricate ideas like distances to work. All manifolds are topological spaces at heart, and this is the setting from which they evolve, but it is usually only necessary to use this detail when investigating abstract unphysical spaces. To be able to physically use the maths, it is best to jump straight to Differentiable Manifolds.

Definition 2 *The definition of a Topological Manifold is a topological space $\mathcal{M}$, that is:*

- *Second Countable - the topology has a countable basis,*
  $\exists\, \mathcal{B} = \{B_i\}_{i=1}^{\infty} : \bigcup_i B_i = \mathcal{M}$ *and*
  $\forall i, j \in \mathbb{N}, \forall x \in B_{i,j} = B_i \cap B_j,$
  $\exists I \subseteq B_{i,j} : x \in I$
- *Hausdorff - Any 2 points in the topology can have disjoint neighbourhoods.*
  $\forall x, y \in \mathcal{M}, \exists$ *open sets* $X, Y :$
  $x \in X, y \in Y$ *and* $X \cap Y = \emptyset$
- *For a cover $\{U_i\}_{i=1}^{m}$ of $\mathcal{M}$, $i = 1 \ldots, n$ with each U_i open, $\exists$ an Atlas $A = \{U_i, \Phi_i\}_{i=1}^{m}, \Phi_i : U_i \to V_i \subseteq \mathbb{R}^n$.*
- *The transition maps, defined as* $\Phi_i^j := \Phi_i \circ \Phi_j^{-1}$ *are homeomorphic, i.e the maps are continuous and have continuous inverses.*

Further, if the transition maps are C^{∞} diffeomorphic, i.e. both they and their inverses are infinitely differentiable, then this is called a Differentiable Manifold.[2]

It is now possible to answer the question posed earlier, "Is a cross a manifold?" Consider Figure 2, here two neighbourhoods of the center point p are shown. These are open, so do not include

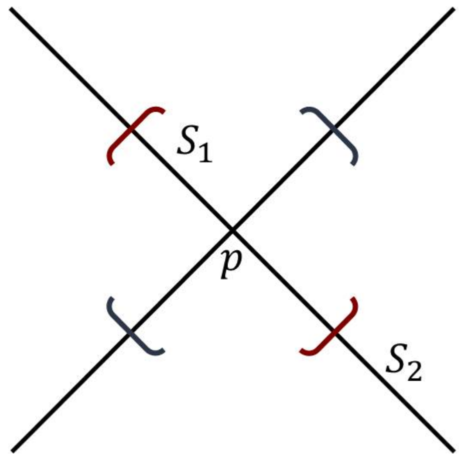

Figure 2: An example of a space that fails to be a manifold, with two neighbourhoods, S_1, S_2, of the point p shown

their boundaries, however the intersection of these two sets, $S_1 \cap S_2 = \{p\}$ is a closed set. Hence this space fails the third condition in Definition 1, is not a topology and therefore not a manifold. This example illustrates the importance of the mathematical rigour in physical systems. It is easy to envisage a system of motion where a particle is confined to a cross, but in this case one must remember that manifold theories will not necessarily apply.

Before proceeding to more study, one more note on the fundamentals of manifolds will be made. This is about the orientability of manifolds. Orientability essentially means the ability to define a consistent coordinate system across the whole manifold. There are several mathematical definitions of this property, but a useful one is as follows:

Definition 3 *Defining the Jacobian matrix of a transition map Φ_i^j as*

$$J_{\mu\nu}^{i,j} = \partial_\nu \Phi_{i\mu}^j, \quad (1)$$

a manifold is defined to be orientable iff $\exists\, A = \{U_i, \Phi_i\}_{i=1}^m : \det(\mathcal{J}^{i,j}) > 0$, $\forall i, j = 1, \ldots, m$ *[3]*

2.1.2 1-D Manifolds

The dimension of a manifold is defined as the dimension of $\mathbb{R}^n$ that the charts Φ_i map to. It thus seems a logical step to look at the lowest dimension manifolds, excluding 0-D manifolds, which are collections of points and will have trivial properties. It can be shown[4] that there are only four distinct, connected 1-D manifolds, all others are diffeomorphic (can be smoothly deformed) to these:

- $[0, 1]$
- $(0, 1)$
- $[0, 1)$
- $\mathbb{S}^1$

Importantly, these are all orientable. This result follows trivially from the first three, since these are just sections of $\mathbb{R}$ which is certainly orientable, and are covered by one chart only, namely the identity, $\Phi(x) = x$. On the other hand, any attempt to cover $\mathbb{S}^1$ by a single chart will fail, since it will either miss points or double cover points, due to the charts being open. An Atlas can be achieved with the two charts $\left(\mathbb{S}^1 \backslash \{N\}, \theta\right)$

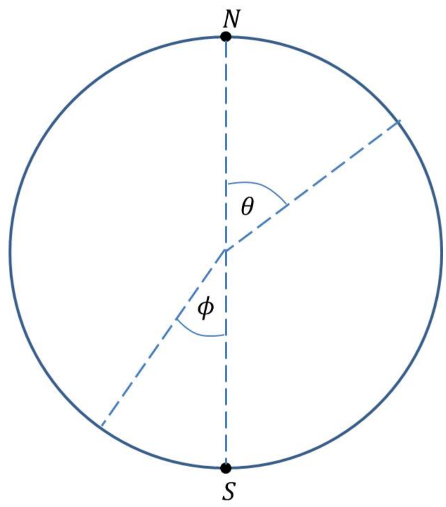

Figure 3: The set $\mathbb{S}^1$ with two compatible charts shown on it.

and $\left(\mathbb{S}^1 \backslash \{S\}, \phi\right)$, with transition map,

$$\phi = \begin{cases} \theta - \pi & \text{if } \theta \in (\pi, 2\pi) \\ \theta + \pi & \text{if } \theta \in (0, \pi) \end{cases}, \quad (2)$$

as in Figure 3.

The Jacobian of this transition map is $\mathcal{J} = (\partial_\theta \phi) = 1 > 0,\ \forall \theta$. So an Atlas is found that has positive Jacobian determinant, by Definition 3 this implies $\mathbb{S}^1$ is also orientable. The use of this result is that any non-intersecting path traced out by a particle, will be orientable.

2.1.3 Tangent Manifolds

The concept of a vector becomes hazy when starting to examine manifolds, the usual understanding is of an object that 'points' from one place to another, but if the surface of a sphere is considered, this concept of pointing no longer makes sense. Either a vector now passes out of and back into the manifold, or else it is curved in some way. Neither of these notions offer a consistent construct, the first requires the notion of a manifold being embedded in a higher dimensional space whilst the second is not defined by a point but by a path. So follows the idea that these 'vectors' must be redefined as existing in some co-dimensional space outside of it. Take a path on $\mathcal{M}$, the manifold, defined as:

$$C := \{\gamma(t) : t \in [0,1]\} \subseteq M, \qquad (3)$$

then at any point on this path, consider the quantity $d_t\left(\Phi_i \circ \gamma\right)(t)$. This is tangent to the motion of the particle and thus to the manifold, so will form the new concept of vector.

Definition 4 *$\gamma : [a,b] \to \mathcal{M}$ is a differentiable curve on $\mathcal{M}$, at the point t_0 if the limit:*

$$\lim_{t \to t_0} \frac{(\Phi_i \circ \gamma)(t) - (\Phi_i \circ \gamma)(t_0)}{t - t_0} \qquad (4)$$

exists and is unique.[5]

Definition 5 *A Tangent Vector at the point $p := \gamma(t_0)$ is then defined as $\gamma'(t_0)$.[6] The set spanned by all Tangent Vectors, generated by all differentiable curves passing through p is called the Tangent Plane at p and is denoted, $T_p\mathcal{M}$.*

With this new understanding of vectors, the framework for the following theory can be created by defining one more set, the Tangent Bundle.

Definition 6 *The Tangent Bundle of $\mathcal{M}$ is defined as*

$$T\mathcal{M} := \bigcup_{p \in \mathcal{M}} T_p\mathcal{M}, \qquad (5)$$

and has a corresponding canonical projection

$$\pi : T\mathcal{M} \to \mathcal{M}, \ \pi(p, v_p) = p \qquad (6)$$

The Tangent Bundle thus contains all of the possible positions and velocities of any particle on the manifold's surface, and it is this property that will prove invaluable when defining Lagrangians later. As a final note, this is a product of two manifolds, $\mathcal{M}$ and its Tangent Planes, and is therefore a manifold in its own right with twice the dimension of the $\mathcal{M}$, i.e. $T\mathcal{M}$ will inherit the differentiable structure and other regular properties of M, a fact also helpful when working with functions defined on it.

2.2 Noether's Theorem

2.2.1 Euler-Lagrange Equations

All of Hamiltonian mechanics is derived from one principle[7]:

$$A(\mathcal{L}) = \int_{t1}^{t_2} \mathcal{L}\, dt, \text{where } \mathcal{L} := T - V, \quad (7)$$

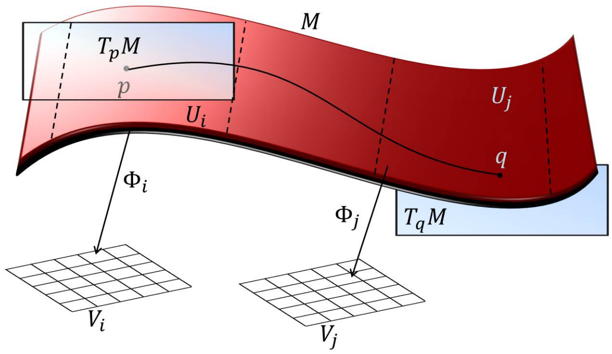

Figure 4: A typical manifold with two charts (U_i, Φ_i) shown, and examples of the Tangent Planes.

the difference of Kinetic and Potential energies. From this principle and the calculus of variations, one arrives at the first great tool in Hamiltonian Mechanics, the Euler-Lagrange equations.

Definition 7 *For a Lagrangian $\mathcal{L}(q_1, ..., q_n, \dot{q}_1, ..., \dot{q}_n, t)$, the Euler Lagrange (E-L) equations are defined as:*

$$\left(\partial_{q_i} - d_t \partial_{\dot{q}_i}\right) \mathcal{L} = 0, \forall i = 1, \ldots, n \tag{8}$$

where the q_i are generalised coordinates. The solution of these equations is the path followed by a system minimising its action.

The usefulness of these equations is best observed with an example. Consider a simple pendulum, with coordinate $\theta(t)$ measured from the vertical, length l, then the height is $l\,(1 - \cos(\theta))$, and the potential energy $mgl\big(1 - \cos(\theta)\big)$. The Lagrangian of this system is:

$$L = \frac{1}{2} ml^2 \dot{\theta}^2(t) - mgl\Big(1 - \cos\big(\theta(t)\big)\Big). \tag{9}$$

By applying the Euler-Lagrange equations, the equation of motion is seen to be:

$$\begin{aligned} -mgl\partial_\theta(1 - \cos(\theta)) - d_t(ml^2\dot{\theta}) = 0 \\ \implies \ddot{\theta}(t) + \frac{g}{l}\sin(\theta) = 0, \end{aligned} \tag{10}$$

which is the familiar pendulum equation.

Clearly, this method has a powerful ability to obtain trajectories, but an important property must be emphasised. This is purely a local equation, since it is about relationships between derivatives, and so can only yield information regarding a point. To obtain the equations of motion, it must be be integrated along some path, which is not always possible in the context of manifolds.

2.2.2 Noether's Theorem On Flat Space

The next step from the E-L equations is the famous Noether's Theorem. To derive it there are several approaches, Noether herself used a group theoretical approach, there exists a full manifold approach which will be seen shortly but the place to start, is with the theorem in flat space.

Definition 8 *For a Lagrangian system $\mathcal{L}(q_i, \dot{q}_i, t)$, a continuous symmetry of the system is defined to be a function $\phi^s : \mathbb{R}^n \to \mathbb{R}^n, \phi^0(q_i) = q_i$ such that $\mathcal{L}(\phi^s(q), \dot{\phi}^s(q), t) = \mathcal{L}(q, \dot{q}, t), \forall s \in \mathbb{R}$, where s is some parameter of the function.[8]*

The theorem then states that if such a symmetry exists in the system, then there exists a conserved quantity, the Noether constant:

$$N(q_i, \phi^s) \coloneqq \sum_{i=1}^{n} \partial_{\dot{q}_i}\mathcal{L} \cdot d_s\phi_i^s(q)|_{s=0}. \quad (11)$$

This can be shown[10] by an exercise in differentiation and application of the E-L equations as follows:
Assume a symmetry as above, then by assumption $d_s\mathcal{L} = 0$, factoring out this derivative yields:

$$\sum_{i=1}^{n}\left(\frac{\partial\mathcal{L}}{\partial\phi_i^s(q)}d_s\phi_i^s(q) + \frac{\partial\mathcal{L}}{\partial\dot{\phi}_i^s(q)}d_s\dot{\phi}_i^s(q)\right) + \partial_t\mathcal{L}d_s(t) = 0 \quad (12)$$

Now, using $\lim_{s\to 0}\phi_i^s(q) = q_i$, utilising the E-L Equation, and using Clairaut's theorem of commutativity of derivatives[9]:

$$\sum_{i=1}^{n} d_t\partial_{\dot{q}_i}\mathcal{L}\cdot d_s\phi_i^s(q) + \partial_{\dot{q}_i}\mathcal{L}\cdot d_t d_s\phi_i^s(q)\Big|_{s=0} + \partial_t\mathcal{L}d_st|_{s=0}$$
$$= d_t\sum_{i=1}^{n}\left(\partial_{\dot{q}_i}\mathcal{L}\cdot d_s\phi_i^s(q)|_{s=0}\right) + \partial_t\mathcal{L}d_st|_{s=0} = 0 \quad (13)$$

Hence if $\mathcal{L}$ is independent of t, or t is independent of s, which is assumed true, then the summation is constant. □

Again it is best to understand this with an example. Take a Lagrangian for two interacting particles in $\mathbb{R}^2$:

$$\mathcal{L} = \dot{\underline{r}}_1^2 + \dot{\underline{r}}_2^2 - V\big(|\underline{r}_1 - \underline{r}_2|\big), \quad (14)$$

with a symmetry of rotations about the origin, i.e.

$$\phi^s(\underline{r}_i) = \begin{pmatrix}\cos(s) & -\sin(s)\\ \sin(s) & \cos(s)\end{pmatrix}\cdot\underline{r}_i \quad (15)$$

Note that this is a symmetry of the above Lagrangian, since rotations will preserve speed and distance, but not direction. Then the Noether constant is

$$N = \sum_{i=1}^{2}\dot{\underline{r}}_i\cdot\begin{pmatrix}0 & -1\\ 1 & 0\end{pmatrix}\underline{r}_i, \quad (16)$$

which, if the position is denoted $\underline{r}_i = (x_i, y_i)$, is

$$N = \sum_{i=1}^{2}\dot{y}_i x_i - \dot{x}_i y_i, \quad (17)$$

and this is familiar as the total angular momentum. This technique can be employed to find several other variables, but the problem remains that this is a theorem based on flat space. When particles are constrained to different manifolds, it is not necessarily true that local constants remain so on a global variable as the example in the introduction demonstrates. To generalise this theorem, Section 2.1.3 must be utilised.

2.2.3 Noether's Theorem On a General Manifold

The problem of extending the theorem to a general manifold, is solved[11] by reducing the manifold back to $\mathbb{R}^n$ via it's charts, and then applying the flat case to this new function. To start this, the Lagrangian must be redefined from a function of coordinates, to a function on the tangent space, $\mathcal{L} : T\mathcal{M} \to \mathbb{R}$. The motivation for this choice was explained earlier, in Section 2.1.3 and it creates a helpful framework for working on manifolds. To perform differentials and other calculations however, there must be composition with charts to generate coordinates. In this sense a "Local Lagrangian" is defined in a specific chart as:

$$\mathcal{L}_i = \mathcal{L} \circ \Phi_i^{-1} : V_i \subseteq \mathbb{R}^n \to \mathbb{R} \tag{18}$$

and from the symmetry $\phi^s : M \to M$, a "local symmetry" is created as

$$\phi^s_{i,j} \coloneqq \Phi_j \circ \phi^s \circ \Phi_i^{-1}, \tag{19}$$

which accounts for the case where the symmetry moves the position from chart i to chart j. Using these quantities, the conserved quantity becomes:

$$N(p, v_p) = \sum_\alpha \frac{\partial \mathcal{L}}{\partial v_p^\alpha} \cdot d_s \left(\phi^s_{i,j}(x^\alpha)\right)|_{s=0} \tag{20}$$

The proof of Equation 20, follows the same route as before but now with objects dependent on the charts. This will cause previously unknown behaviour when the symmetry alters the path of a particle into a different chart, and specifically with differentials of the local symmetry. This is one of the problems that among other examples, the Möbius strip faces, and one that forms a key part of the investigation.

3 Methodology

The first approach taken in this project was to test the strengths and limitations of the flat case of Noether's theorem by applying it to several Lagrangians and symmetries. The scheme for this was to consider a system, construct a Lagrangian based on energy calculations, then to determine the symmetries. This last part posed problems, since there appeared to be no simple way to find these symmetries. The method employed was to systematically test symmetries of just one variable, then to move on to two variable symmetries, then three etc. These multi-variable symmetries tended to be of similar form to angular momenta, i.e. cross products of positions and velocities, so it was generally this form of symmetry that was tested.

The study then moved to research into Manifolds. This involved proving results, such as the existence of only four distinct 1-D manifolds. These proofs were generally via constructive arguments, i.e. creating Atlantes, testing their behaviour and using logical arguments to say that other Atlantes are equivalent so the specific result can be generalised. An proof was found[11], regarding the generalisation of Noether's theorem to general manifolds however the original syntax contained many errors so rewriting this became a primary task, and in the process understand when the theorem would not work.

After a better understanding of these theories had been established, the investigation branched into three sections studying motion on specific manifolds. The first case was the cylinder $\mathbb{S}^1 \times \mathbb{R}$. A Lagrangian for the system was created, made chart specific and then equations of motion were obtained by utilising the E-L equations and Noether's. Different potentials were tested, taking into account that the distance function will be dependent on the space, in the case of the cylinder the distance between points is no longer generated from a unique path. The potentials that this led to were sketched and their behaviour, differentiabilty and symmetries were examined to deem which would be best in a Lagrangian.

The sphere, $\mathbb{S}^2$ was studied next. The Lagrangian was created by assuming the

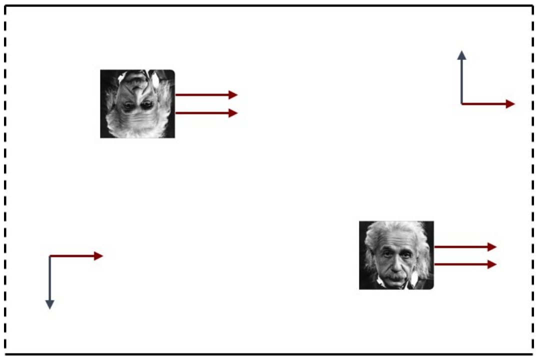

Figure 5: In this diagram, the reversal of the coordinate system is demonstrated, due to the non-orientability of the Möbius strip.

Cartesian form, switching to spherical polar co-ordinates and then restricting the motion to the surface of the sphere after. A Noether's constant was found, and its dependencies studied, the equations of motion were obtained and examined numerically with Mathematica, then inferred that they were the geodesics of the sphere. A short investigation followed to determine whether the paths of free motion on any manifold were the geodesics.

Lastly the Möbius strip was studied, one approach was to use the Manifold version of Noether. By attempting this, the problem of defining a Lagrangian became clear. A new approach entirely was tried. The problem was seen as one of continuity, since the perpendicular component of momentum flips from one direction to another discontinuously in the classical Möbius strip. Complexification of the perpendicular coordinate led to new analysis and by application of E-L and Noethers, equations of motion were obtained. Feedback was given to the initial Lagrangian, which was subsequently altered to gain reasonable results. A constant of motion was found and an equation for the complex coordinate was analysed via a phase plane. Distance functions were then examined, similar methods to the cylinder were used, and the functions plotted in Mathematica. The symmetries of these functions were investigated to determine which would leave constants of motion intact. Finally, the Möbius was briefly studied as a constrained system in $\mathbb{R}^3$ and the form of a constraint force was generated.

4 Results

The results will be split in four sections, firstly an important general result of Noether's theorem, then move on to specific results pertaining to the three significant manifolds studied.

4.1 Results of Manifolds

It was shown that the Noether constant defined in Equation 11, is independent of the coordinate system placed, i.e.

For $y_i = f(\underline{x})$,

$$N(y) := \sum_{i=1}^{n} \partial_{\dot{y}_i}\mathcal{L}\, \dot{d}_s\phi^s(y_i) = \sum_{i=1}^{n} \partial_{\dot{y}_i}\mathcal{L}\, \dot{d}_s\phi^s(y_i) = N(x) \quad (21)$$

This means that if a constant is found with one chart, it will be found in all other charts, so general results follow from chart specific results.

4.2 Cylinder

The first non-trivial manifold that was experimented with was the cylinder, $\mathbb{S}^1 \times \mathbb{R}$. The charts that cover it are easily found by extending Equation 2. Three conserved quantities were found on it using Noether's, a momentum around the cylinder, one along it and a locally conserved angular momentum. The starting point for all three of these was the free cylinder Lagrangian:

$$\mathcal{L}_{cylinder} = \dot{\theta}^2 + \dot{z}^2, z \in \mathbb{R}, \quad (22)$$

which was simply derived from an understanding of the kinetic energies present in Angular Mechanics. The first two conserved quantities were to be expected, the third takes the form $\dot{z}\theta - \dot{\theta}z$, and can be seen that it should exist, since the cylinder is very similar to flat space, except for an association at the ends.

The main problem that arises with this Manifold and the reason it was chosen to study was when defining potentials. Since the distance between any two points is now dependent on which route is taken, the first distance function was defined as the shorter of the two routes:

$$\mathrm{d}(1,2) = \begin{cases} \sqrt{\Delta\theta^2 + \Delta z^2} \\ \text{if } |\Delta\theta| \le \pi \\ \sqrt{(2\pi - |\Delta\theta|)^2 + \Delta z^2} \\ \text{if } |\Delta\theta| > \pi \end{cases}, \tag{23}$$

which causes it to lose its differentiability when the points are antipodal, $\Delta\theta = \pi$, as seen in Figure 6. A potential of the form $V(1,2) = (\mathrm{d}(1,2))^{-1}$ this predicts that particles will reach a minimum energy when antipodal. Another way to define the distance takes inspiration from the concept of fields permeating through space. This leads to the idea that on a cylinder the field will permeate in two directions to the same point, thus any potential will be the sum of these two contributions, i.e for an inverse square force, this means an inverse potential and so defining the distance as

$$\mathrm{d}'(1,2) = \left(\left(\Delta\theta^2 + \Delta z^2\right)^{-\frac{1}{2}} + \left(2\pi - |\Delta\theta|\right)^2 + \Delta z^2\right)^{-\frac{1}{2}}\right)^{-1}, \tag{24}$$

allows $V(1,2) = \left(\mathrm{d}'(1,2)\right)^{-1}$ to seem reasonable, and regains differentiability, an important property in Lagrangian theory.

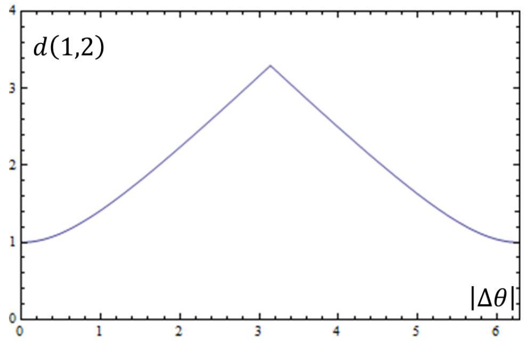

Figure 6: This graph shows the distance between two points on a cylinder with $\Delta z = 1$

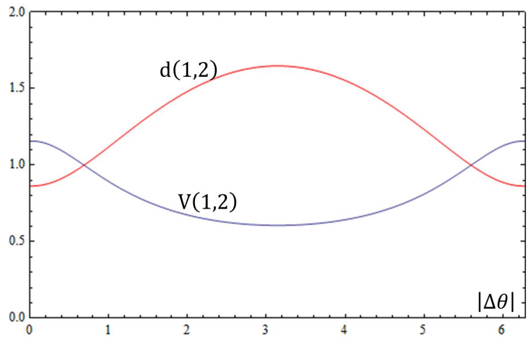

Figure 7: This graph shows a different distance function and its corresponding potential on a cylinder with $\Delta z = 1$

4.3 Sphere

For a sphere, $\mathbb{S}^2$, it was shown that it cannot be covered with only one chart, and examples were constructed for compatible charts that will cover it. One such Atlas was a set of two stereographic projections, here the Northern map is defined as a function of Cartesian coordinates (x, y, z):

$$\Phi_N(p) = \Phi_N(x,y,z) = (X_N, Y_N) = \left(\frac{-x}{1-z}, \frac{y}{1-z}\right) \tag{25}$$

As can be seen this map becomes undefined at the north pole, $z = 1$, so does not completely define a manifold, but together with one undefined on the South Pole, Φ_S allows the sphere to be covered, it is a simple exercise to demonstrate that the transition map is diffeomorphic (see Definition 2), function. A result from using this map is that the determinant of the Jacobian is

$$\det \mathcal{J}(\Phi_S \circ \Phi_N)(X_N, X_S) = \frac{1}{X_N^2 + X_S^2} > 0, \forall (X_N, X_S) \in \mathbb{R}^2, \quad (26)$$

and therefore by Definition 3, the sphere is orientable. This was the main result obtained from this Atlas, it was then decided to move onto a more classical Atlas, the spherical polar coordinate system. This coordinate system is spanned by $(\theta_1, \varphi_1) \in (0, 2\pi) \times (0, \pi)$ and contains singularities at $\theta = 0$, and $\phi = 0, 2\pi$. These limitations are not detrimental however as together with a different chart, (θ_2, φ_2) rotated by π in both the θ_1 and φ_1 directions, an Atlas is created. The technique of embedding the Sphere in $\mathbb{R}^3$ was used as a stepping stone to arrive at a Lagrangian, since the Lagrangian is well known in this flat space. From there substitution, and thus restriction to the surface, was made and the Lagrangian was determined to be:

$$\mathcal{L}_{sphere} = \dot{\varphi}_i^2 + \sin^2(\varphi_i)\,\dot{\theta}_i^2, \quad (27)$$

At this point it was time to employ Noether. It was seen that,

$$\phi^s(\theta_i, \varphi_i) = (\theta_i + s, \varphi_i) \quad (28)$$

was a symmetry of $\mathcal{L}_{sphere}$, this led to

$$N = \sin^2(\varphi_i)\dot{\theta}_i \quad (29)$$

being the conserved quantity. What this implies is that as a particle tends to the poles the speed $\dot{\theta}_i$ will tend to ∞. It can then be proved that no other continuous symmetries are present in the $\mathcal{L}$, since any other symmetry will have to be symmetric over $\sin(\varphi_i) \implies \phi^s(\varphi_i) = \varphi_i$, i.e. the trivial symmetry. Not much more was able to be done, since the motion of two coordinates cannot be solved with just one equation. Another was obtained from the E-L for θ,

$$\ddot{\varphi}_i = \sin(\varphi_i)\cos(\varphi_i)\dot{\theta}_i^2 \quad (30)$$

Combining these two led to a 2^{nd} order ODE:

$$\ddot{\varphi}_i = N^2 \frac{\cos(\varphi_i)}{\sin^3(\varphi_i)} \quad (31)$$

This is analytically unsolvable, so Mathematica was utilised to numerically solve and plot graphs of the motions, which can be seen in Figures 8 and 9. The observation here is that the two angles vary out of phase with each other, this was initially thought to be particles

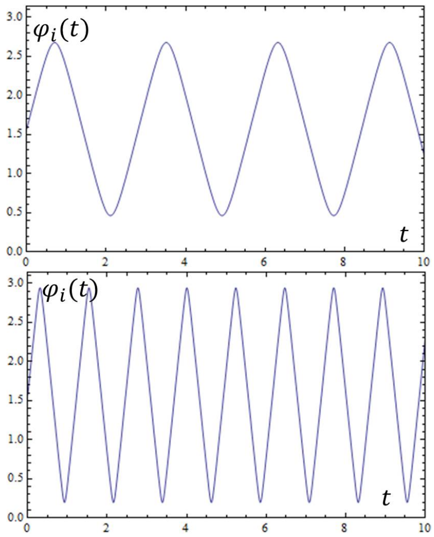

Figure 8: These graphs demonstrate the time evolution of the polar angle for a free particle on the sphere $\mathbb{S}^2$, with initial speeds $\dot{\varphi}_i(0) = 5$ and 2 and $\dot{\theta}_i(0) = 1$

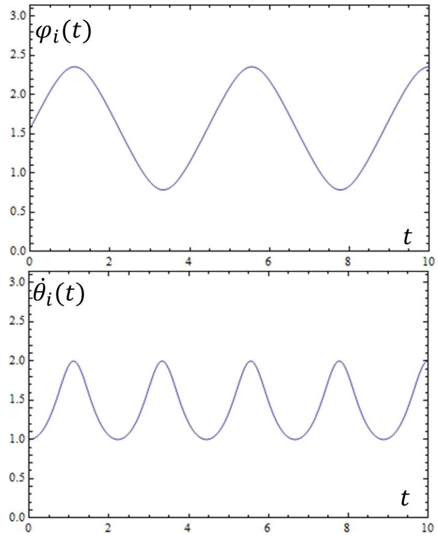

Figure 9: These graphs demonstrate the time evolution of the polar angle and the azimuthal speed for a free particle on the sphere $\mathbb{S}^2$, with an initial speed $\varphi_i(0) = 1$ and $\dot{\theta}_i(0) = 1$

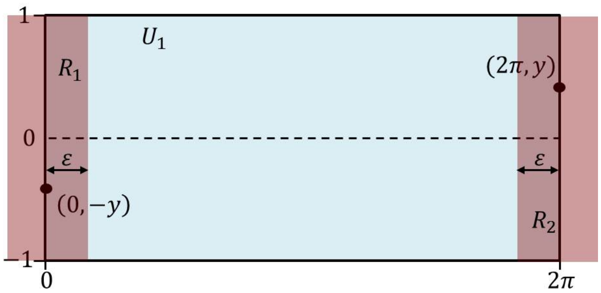

Figure 10: This Figure displays the Möbius strip, $(0, 2\pi) \times (-1, 1)/{\sim}\ (2\pi, y) {\sim} (0, -y)$, with an Atlas shown on it.

oscillating around the equator, but soon it was realised that this was the paths of great circles, those circles on the sphere that have the origin as their centre. The last topic breached with the sphere, was to try and define potentials on it. This essentially required the distance function for a sphere, i.e. for a great circle, which is well documented, and can be calculated as

$$\mathrm{d}\big((\theta^1, \varphi^1), (\theta^2, \varphi^2)\big)$$
$$= c^{-1}\left(c(\varphi^1)c(\varphi^2) + s(\varphi^1)s(\varphi^2)c(\Delta\theta)\right), [12] \tag{32}$$

where c = cos and s = sin. This is symmetric over the symmetry in Equation 28, so the conserved quantity in Equation 29 will remain (or some equivalent summation for multi particle cases), in any system with a Lagrangian of the form $\mathcal{L} = \sum_{i,j} T(p_i) - V(d(p_i, q_j))$.

4.4 Möbius Strip

The Möbius strip is defined as $(0, 2\pi) \times (-1, 1)$ with an equivalence relation: $(2\pi, y) \sim (0, -y)$. The first exercise was to create an Atlas for this, for which it was observed that the Möbius behaves exactly as $\mathbb{R}^2$, except for a single line, leading to the obvious choice for an atlas :

$$A = \Big((U_1, \Phi_1), (R_1 \cup R_2, \Phi_2)\Big)$$
$$U_1 = (0, 2\pi) \times (-1, 1)$$
$$R_1 = (0, \varepsilon) \times (-1, 1)$$
$$R_2 = (2\pi - \varepsilon, 2\pi) \times (-1, 1) \quad (33)$$

demonstrated clearer in Figure 10, with transition map defined as,

$$\Phi_2 \circ \Phi_1^{-1}(x, y) = \begin{cases} (x - (2\pi - \varepsilon), y) \\ \quad \text{if } (x, y) \in R_2 \\ \quad (x + \varepsilon, -y) \\ \quad \text{if } (x, y) \in R_1 \end{cases}. \quad (34)$$

It was shown that the Jacobian determinant of this transition map is -1 and by arguing that any other combination of maps will be simplified to these two, the Möbius is proved to be non-orientable. This result is the incentive for researching this manifold. The next result obtained was an application of the proof described in Section 2.2.3. In this proof the conserved Noether quantity begins has dependence on $d_s\phi^s_{i,j}$, defined in Equation 19, so the constant becomes dependent on the derivative $d_s(\Phi_j \circ \Phi_i^{-1})$ and thus the Jacobian determinant becomes a factor. This leads to the idea that on the Möbius, the Noether constant is no longer constant for the perpendicular momentum. It is however true, by the orientability of 1-D manifolds, that the path taken by the particle will be conserved in a free system.

This result, although helpful, does not lead to equations of motion and trouble is seen if a Lagrangian is defined. The first attempted was:

$$\mathcal{L} = \dot{x}^2 + \dot{y}^2. \quad (35)$$

The trouble with this is that it does not encapsulate any information about the Möbius' twisting nature, and the "flipping" of the momentum is expected to happen discontinuously when a particle crosses the line $x = 0$. This problem of a discontinuous equation of motion inspired the thinking of treating one of the coordinates as if it were not stuck in $\mathbb{R}$ but instead in $\mathbb{C}$. This allows the perpendicular coordinate, from now on called $z(t)$, to rotate continuously from one point to another, and if the argument of z is dependent on x, this still leaves only 2 independent parameters $|z|$ and x, this was initially set up as:

$$z(x, t) = z_0(t)e^{i\theta(x)}, \text{b.c } \theta(2\pi) = \theta(0) + \pi \quad (36)$$

It seems fair to note now that throughout this analysis, all results must tend to those of a flat system in the limit of no rotation, termed the "flatness condition". The next step from here was to define a Lagrangian of this system. Free Lagrangians generally have the form of the speed squared, so it seems a reasonable assumption to let:

$$\mathcal{L}_{complex} = |\dot{z}|^2 + \dot{x}^2 \qquad (37)$$

However since z has dependence on x, this is not a function of two independent parameters. Expanding out $|\dot{z}|^2$ yields, $\dot{z}_0^2\theta'^2(x)z_0^2\dot{x}^2$, so in fact the Lagrangian is best defined as:

$$\mathcal{L}_{complex} = \dot{z}_0^2 + (1 + f'^2(x)z_0^2)\dot{x}^2, \qquad (38)$$

which obeys the flatness condition. This appears an odd choice at first, since it affects the x term rather than the z_0, but when one considers the increased dependence on x of the velocities it makes more sense, if not particularly usual. The next step as usual is then to start using the two variational theorems, firstly Noether. The symmetries of this Lagrangian seem hard to obtain at first, so it is best to attack case-wise. Firstly, symmetries of the form $\phi^s(z_0, x) = (\phi^s(z_0), x)$. It is quickly determined, by the same logic as the sphere, that this must be a symmetry of $f'^2z_0^2$, i.e. only the trivial symmetry holds. For a symmetry, $\phi^s(x)$, the relations

$$d_t\phi^s(x) = \dot{x} \text{ and } f'(\phi^s(x)) = f'(x) \qquad (39)$$

must hold, which imply that $\phi^s(x) = x + s$ and $f'(x) = f'(x+s)\ \forall s \in \mathbb{R}$. So a symmetry exists if $f(x) = \omega x$, i.e. a smooth rotation. The corresponding conserved quantity is :

$$N = \dot{x}(1 + \omega^2 z_0^2), \qquad (40)$$

which is the standard x-momentum in the flatness condition. After finding the one conserved quantity, another equation of motion is obtained from the E-L of z_0:

$$\ddot{z}_0 = 2\omega^2\dot{x}^2 z_0, \qquad (41)$$

so by combing these two results, it is found that the equation of motion for z_0 is:

$$\ddot{z}_0 = 2\omega^2 N^2 \frac{z_0}{(1+\omega^2 z_0^2)^2}. \qquad (42)$$

This equation was analysed by its phase plots, as seen in Figure 11. Here it is seen that for small speeds, the direction of motion will switch, whilst for large it will remain constant. This can be explained as small velocities correspond to the particle moving up the strip, and low velocities mean that the other component will be dominant and the particle will move round the strip. Potentials on the Möbius were then looked at, for the real case. Similarly to the cylinder the problem of distance came into play, and borrowing from the cylinder were two different choices of distance, one that follows the shortest route and the other that is a combination of the two routes, as in Equations 23 and 24, the only differences being that now the

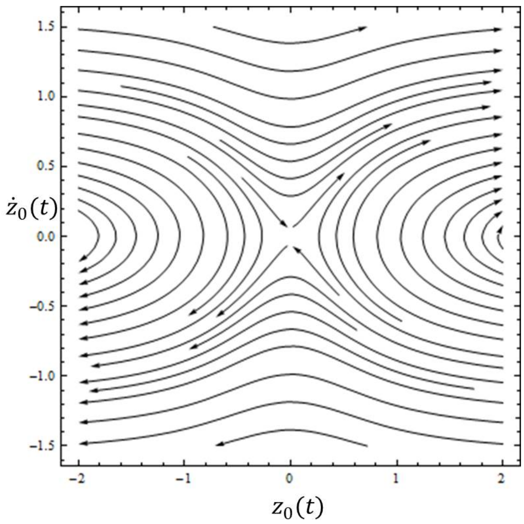

Figure 11: This shows the phase diagram for the complex amplitude of a particle moving on a Möbius strip.

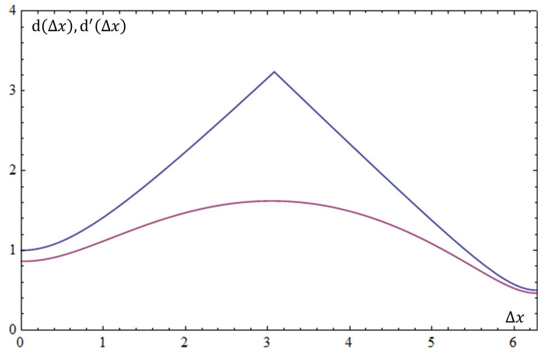

Figure 12: This shows two possible distance functions defined on the Möbius strip. The upper being the minimum path length, and the other being a combination.

value of the perpendicular separation Δy (note: Δz on the cylinder) is dependent on the route taken, and secondly that the critical point of the two routes being equal length is no longer π but instead, is dependent on the y position. The first choice of distance is:

$$\mathrm{d}(1,2) = \begin{cases} \sqrt{\Delta x^2 + \Delta y^2} \\ \text{if } \Delta x \leq \pi + \dfrac{y_1, y_2}{\pi} \\ \sqrt{(2\pi - \Delta x)^2 + (\mathbf{y_2} + \mathbf{y_1})^{\mathbf{2}}} \\ \text{otherwise.} \end{cases} \tag{43}$$

and by labelling the top and bottom functions in Equation 43, d_1 and d_2 respectively, the other distance can be defined as:

$$\mathrm{d}'(1,2) = \left((\mathrm{d}_1(1,2))^{-1} + (\mathrm{d}_2(1,2))^{-1}\right)^{-1}. \tag{44}$$

In Figure 12 the two distances are graphed, with $y_1 = -0.25, y_2 = 0.75$ fixed. The merits of each function can be seen, d' is differentiable, which makes it a good candidate for use in Lagrangians, whilst the other represents a more conventional form of distance. The last point of study in this project was to investigate embedding of the strip in $\mathbb{R}^3$, and observing Newtonian forces. It was envisaged that it could be constructed by a plane being rotated around a co-moving pivot, so the force felt at a point on the strip would be centripetal, and defining the angle made by the plane to the z direction as α, would take the form:

$$\underline{F} = \dot{\alpha}^2(\underline{c}(\alpha) - \underline{r}), \tag{45}$$

where the centre of rotation is $\underline{c}(\alpha)$, and it's gradient determines the twisting of the strip. This force thus contains two components, a standard force causing rotation about the origin, and another component that can be interpreted as a restraining force.

5 Discussion

From the basic Hamiltonian theory established in Section 2 a lot has been built up. An early result was found, regarding the invariance of constants under coordinate transformations, seen in Section 4.1, which allows coordinate specific constants to generalise to global constants. By inclusion of Manifold theory it then became possible to generalise Noether's theorem to various spaces, and to demonstrate when her theory breaks down, as seen in the case of the Möbius strip in Section 4.4. The decision to handle this inclusion in three sections, regarding the three Manifolds deemed fundamental allowed the theory to grow gradually and provided structure to the investigation.

Starting with the Cylinder in Section 4.2, some examples of Noethers theorem being applied were seen and constants of motion were produced, two momenta and a local angular momentum, and their domains in which they remained constant were discussed. This is the first example of a Lagrangian system where more than one chart was required, a fact most people tend to neglect, and by doing the Manifold study, it was seen why it is reasonable to neglect this consideration. Potentials on the cylinder were then discussed, and an important concept was introduced, the idea there is more than one route for a radial force to reach a point. This led to equilibria positions being established, when particles were antipodal, where in flat space there would be none, and thus the concept that changing the structure of the space, changes the behaviour of interacting particles.

The study then moved onto the Sphere in Section 4.3 where it was found there was only one conserved quantity, the sphere-momentum, in a specific chart, despite original thoughts that there would be two. This constant, seen in equation 29, demonstrated the collapse of Flat Noether theory when particles reached the poles, as their speeds became infinite. The creation of two compatible maps then creates the two expected conserved quantities, corresponding to orbits through the poles and orbits around the equator, but generated in different charts. The equations of motion were found for a free particle system and generated, these were interpreted to be the Great Circles, the geodesics of the sphere. Lastly distances were discussed on the sphere, a standard result, and it was observed that this function retained the symmetry of the Noether quantity, meaning that for multi particle systems, with interacting potentials as functions of distance, there will still exist a Noether constant, defined as a sum of the individual sphere-momenta.

The last section, section 4.4, involved the most abstract space to set Noether's theorem, this demonstrated an extreme case of the breakdown. Even though the Möbius behaved as $\mathbb{R}^n$ for most of the space, it's fundamentally non-orientable nature, caused the loss of one of the momenta. By replacing one of the coordinates with a complex variable, it was shown that a new constant of motion emerged in a specific case of constant curvature, seen in equation 40, which is to be expected by the orientability of the path. Utilising this and an Euler-Lagrange equation obtained an ODE for the magnitude of this complex coordinate. This was analysed by method of phase diagrams, figure 11 and expected behaviour was seen, with small z_0 velocities, the direction of motion switched, since the particle would pass around the strip, and for large velocities the particle would retain its motion.

6 Conclusions

6.1 Physical Applications

This abstract study may seem just a curiosity when first viewed, but it does lead to some potential applications. The sphere and cylinder are manifolds that are often realised in nature, e.g. motion on the Earth or the magnetic field around a wire, whilst the Möbius is something not yet seen.

The predictions of this paper are that if a non-orientable region of space existed then particles could enter into it and return with their direction of motion being switched. This would most likely be interpreted as some force existing, but as general relativity demonstrates, forces can merely be manifestations caused by changes in geometry. This geometrical effect could be distinguished from a physical force with the help of neutrinos. Since they have only been observed existing as left-handed[14], if a right-handed were observed emerging after changing its direction of travel then it could provide evidence for non-orientable regions of space.

The other possible application is an idea outlined in Dr. Hadley's paper, The orientability of spacetime[13]. In this, Hadley argues that the inclusion of a time non-orientable region of space-time leads to particle antiparticle pair creation/annihilation. The properties of the Möbius and the creation of the complex Lagrangian outlined in this paper, argue that within the region, the particle will not immediately "flip" to its antiparticle but will gradually transition and whilst within the non-orientable region will be in a superposition of the two states. This exciting prediction is something commonly seen in Quantum

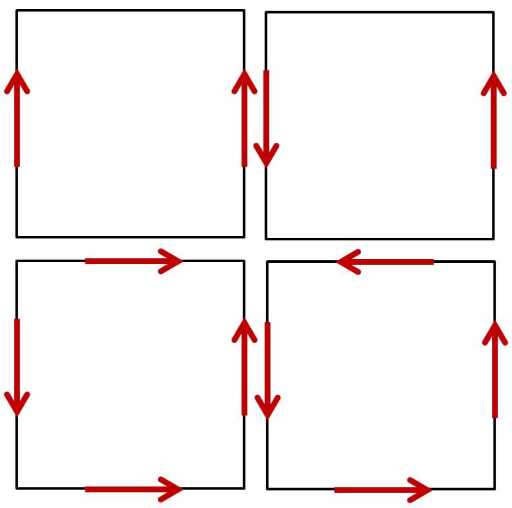

Figure 13: This Figure shows the fundamental polygons (arrows denote equivalence principles) for the Cylinder, Möbius strip, Klein Bottle, Real Projective Plane (From Top Right to Bottom Left).

Theory, so it is possible that many of the ideas expressed in Quantum Theory, could be just manifestations of abstract space-time manifold.

6.2 Further Study

To extend the results displayed, the first step would be to invoke field theory and thus Lagrangian densities, $\mathscr{L}$:

$$\mathcal{L} = \int_{\mathbb{R}^3} \mathscr{L} dV. \tag{46}$$

The main problem foreseen to arise with this extension is that a field forms a continuum over the manifold, e.g. for a probability distribution there will always be a probability that a particle exists on the boundary of a chart. This may lead to trouble when defining local potentials and local Lagrangians in chart specific coordinates, and thus will make calculations more challenging to compute.

This theory could also use experimentation on other abstract manifolds, e.g. the Klein bottle, (similar to the Möbius but with the two other sides associated as in the cylinder), the real projective plain (the Klein Bottle with all sides associated as in the Möbius), and higher dimensional Möbius-type spaces. The problems seen with these would be that no longer would physical intuition help since none of these are embeddable in $\mathbb{R}^3$, from here on out the maths would need to do the talking.

Acknowledgments

I would like to thank Dr. Mark Hadley for his guidance and for the many hours he gave up to spend discussing Möbius strips. I would also like to thank David Carvalho for his companionship and ingenious thinking when we felt stuck not knowing where to go. Lastly, I would like to thank Dr. Jim Robinson for his help provided with the smooth running of this project.

References

[1] *Invariant Variational Problems*, E.Noether: Translated by D. H. Delphenich, Nachrichten der Königlichen Gesellschaft der Wissenschaften zu Göttingen, Math.-phys. Klasse, p235-257 (1918)

[2] *Manifolds and Differential Geometry*, J. M. Lee, Graduate Studies in Mathematics, **107**, p4-7 (2009)

[3] *An Introduction to Manifolds, 2nd ed.*, L. Tu, Universitext Springer, 233 Spring Street, New York, NY, USA, p245 (2010)

[4] *Topology from the Differentiable Viewpoint*, J. Milnor, The University Press of Virginia, Charlottesville, p55 (1965)

[5] *Manifolds, Tensor Analysis and Applications 3rd ed*, J. Marsden, T. Ratiu, R. Abraham, California Institute of Technology, Pasadena California, p141-142 (2002)

[6] *A Short Course in Differential Geometry and Topology*, A.S Fomenko & A.T.Mishchenko, Faculty of Mechanics and Mathematics,Moscow State University, p81-86 (2009)

[7] *On a General Method in Dynamics*, W.R. Hamilton, Philosophical Transactions of the Royal Society, p247-308 (1834)

[8] *Mathematical Methods of Classical Mechanics, 2nd ed.*, V.I.Arnold, Graduate Texts in Mathematics, p88 (1978)

[9] *Multivariable Calculus 7th ed.*, James Stewart, McMaster University, p931 (2012)

[10] *Mechanics, From Newton's Laws to Deterministic Chaos, 5th ed.*, F. Scheck, Universität Mainz, Institut für Physik, Mainz, Germany, p115 (2010)

[11] *A Comment on the Proof of Noether's Theorem on Smooth Manifolds*, Q. de Souza, Revista de Fisica, **16**, p4, (1986)

[12] *Direct and Inverse Solutions of Geodesics on the Ellipsoid With Application of Nested Equations*, T. Vincenty, DMAAC Geodetic Survey Squadron, **23**, p88-93 (1975)

[13] *The Orientability of Spacetime*, M. Hadley, Class.Quant.Grav. **19**, p4565-4572 (2002)

[14] *Theory of Neutrinos: A White Paper* R.N. Mohapatra (Group Leader), University of Maryland, USA, SLAC-PUB-11622 (2004)